

SCIENTIFIC REPORTS



OPEN

Global and regional trends of atmospheric sulfur

Wenche Aas¹, Augustin Mortier², Van Bowersox³, Ribu Cherian⁴, Greg Faluvegi⁵, Hilde Fagerli², Jenny Hand⁶, Zbigniew Klimont⁷, Corinne Galy-Lacaux⁸, Christopher M. B. Lehmann⁹, Cathrine Lund Myhre¹, Gunnar Myhre¹⁰, Dirk Olivié², Keiichi Sato¹¹, Johannes Quaas⁴, P. S. P. Rao¹², Michael Schulz², Drew Shindell¹³, Ragnhild B. Skeie¹⁰, Ariel Stein¹⁴, Toshihiko Takemura¹⁵, Svetlana Tsyro², Robert Vet¹⁶ & Xiaobin Xu¹⁷

Received: 28 June 2018

Accepted: 5 December 2018

Published online: 30 January 2019

The profound changes in global SO₂ emissions over the last decades have affected atmospheric composition on a regional and global scale with large impact on air quality, atmospheric deposition and the radiative forcing of sulfate aerosols. Reproduction of historical atmospheric pollution levels based on global aerosol models and emission changes is crucial to prove that such models are able to predict future scenarios. Here, we analyze consistency of trends in observations of sulfur components in air and precipitation from major regional networks and estimates from six different global aerosol models from 1990 until 2015. There are large interregional differences in the sulfur trends consistently captured by the models and observations, especially for North America and Europe. Europe had the largest reductions in sulfur emissions in the first part of the period while the highest reduction came later in North America and East Asia. The uncertainties in both the emissions and the representativity of the observations are larger in Asia. However, emissions from East Asia clearly increased from 2000 to 2005 followed by a decrease, while in India a steady increase over the whole period has been observed and modelled. The agreement between a bottom-up approach, which uses emissions and process-based chemical transport models, with independent observations gives an improved confidence in the understanding of the atmospheric sulfur budget.

There have been large changes in the global and regional SO₂ emissions over the last decades. After a steady increase in emissions of SO₂ since the beginning of the twentieth century¹, the growing awareness of the negative effects of air pollution on environment and human health, gave rise to international and national legislation on emission-reductions^{2–4}. European and North American SO₂ emissions were reduced by 70–80% since 1990^{2,3,5}, with the largest emission reductions in North America occurring in the last part of the period^{1,3,6–8}, while in Europe the reductions were largest in the first part of the period^{1,2,5,9–12}. There were also substantial reductions earlier, from 1980–1990¹. These large regional SO₂ emission reductions resulted in a global decrease from around 1980 until 2000¹, after which the global emissions increased due to a sharp rise in the Chinese emissions up to around 2006, followed by a declining global trend, mainly due to stricter emission controls in China^{13–20} and trends in Europe and North America^{1,4,12,14}. Not all countries have implemented effective emission controls. In India, the emissions continue to increase^{1,21,22}, and India is now the world's second largest SO₂ emitting country after China²³.

¹NILU -Norwegian Institute for Air Research, Kjeller, Norway. ²Norwegian Meteorological Institute, Oslo, Norway. ³QA/SAC Americas, WMO/GAW, Champaign, IL, USA. ⁴Institute for Meteorology, Universität Leipzig, Leipzig, Germany. ⁵NASA Goddard Institute for Space Studies and Center for Climate Systems Research, Columbia University, New York, USA. ⁶Cooperative Institute for Research in the Atmosphere, Colorado State University, Fort Collins, CO, USA. ⁷International Institute for Applied Systems Analysis (IIASA), Laxenburg, Austria. ⁸Laboratoire d'Aérodologie, Université de Toulouse, CNRS, UPS, Toulouse, France. ⁹National Atmospheric Deposition Program (NADP), Champaign, IL, USA. ¹⁰Center for International Climate and Environmental Research – Oslo (CICERO), Oslo, Norway. ¹¹Asia Center for Air Pollution Research (ACAP), Niigata, Japan. ¹²Indian Institute of Tropical Meteorology, Pune, India. ¹³Nicholas School of the Environment, Duke University, Durham, NC, USA. ¹⁴Air Resources Laboratory, NOAA, MD, USA. ¹⁵Research Institute for Applied Mechanics, Kyushu University, Fukuoka, Japan. ¹⁶Environment and Climate Change Canada, Toronto, Canada. ¹⁷Chinese Academy of Meteorological Sciences, Key Laboratory for Atmospheric Chemistry, China Meteorological Administration, Beijing, China. Correspondence and requests for materials should be addressed to W.A. (email: waa@nilu.no) or A.M. (email: augustinm@met.no)

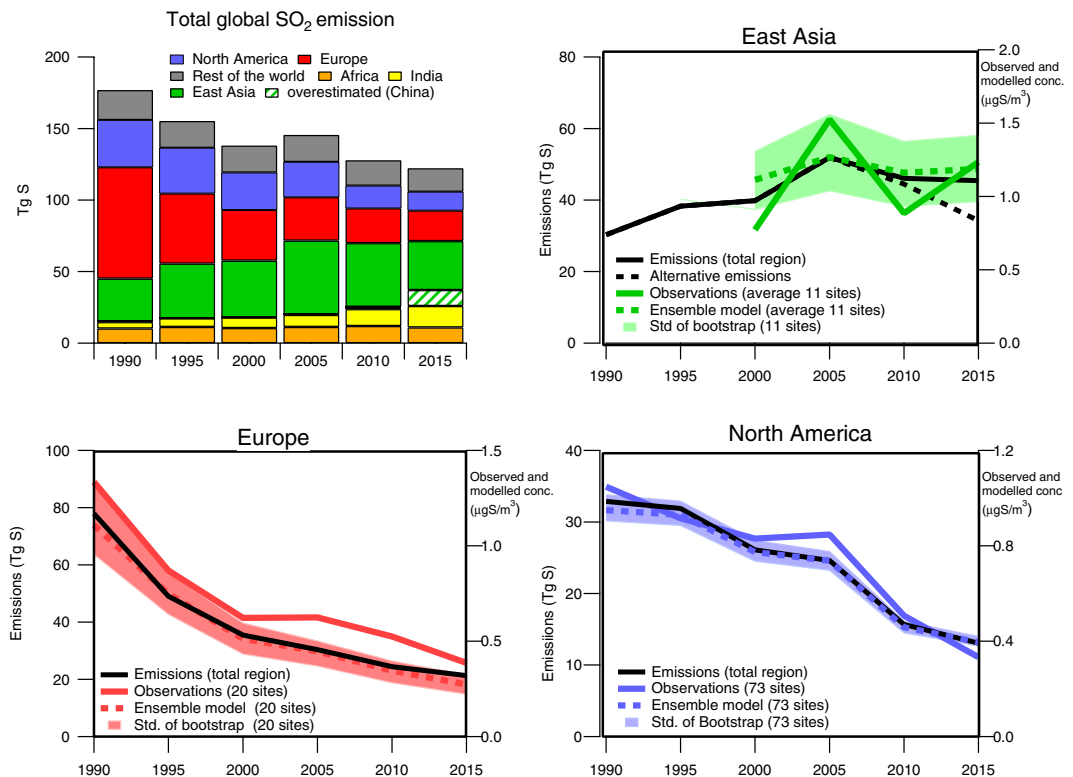


Figure 1. Ensemble modeled and observed trends of sulfate in aerosols over the period 1990–2015 compared to the trend in emissions over the same period. The upper left panel includes a striped green part indicating possible overestimated emissions in China, and the dotted black line in the East Asia panel shows an alternative emission trend adjusted from more recent inventories^{18,20}. The time series show the annual values for years given. The uncertainty is illustrated using the standard deviation of the bootstrap trend for each region.

The large changes in SO_2 emissions have also influenced the radiative forcing of aerosols. Sulfate aerosols have an impact on climate directly by scattering solar radiation and thus cooling the earth's surface, and also an indirect effect on the formation of clouds and precipitation²⁴. The global mean radiative forcing, due to aerosol changes over the 1990–2015 period, increased by about $+0.1 \text{ W m}^{-2}$, but the uncertainty is large²⁵. The main reason for the increased positive radiative forcing of aerosols over this period is the substantial reduction of global mean SO_2 emissions coupled with higher black carbon emissions²⁵. Furthermore, the reductions of SO_2 emissions over Europe are simulated to exert a local radiative forcing of $3\text{--}4 \text{ W m}^{-2}$ for the same period²⁵.

The trends calculated by the global aerosol models have seldom been compared to trends in observations. Trend assessments have mostly been done on regional and national observations^{6–8,11,26,27}, though there are also studies which combine modeled and observed trends^{9,10,28–30}. Global or hemispheric assessments have on the other hand, been done for short time periods or selected years only^{31–35}, or on somewhat limited dataset³⁶ and few models¹⁹. In this study, we have compiled monthly average mean concentrations of SO_2 , sulfate in aerosols and wet deposition of sulfate from major regional networks from 1980 onward until 2015 when available (See Fig. S1 in Supplementary Material (SM)). These trends have been compared to trends estimated by different global models for the period 1990–2015.

We address the question whether global climate models are able to reproduce the recent observed changes in the regional amplitudes of atmospheric sulfur and its inhomogeneous spatial distribution. Reproduction of historical atmospheric pollution levels is crucial to demonstrate that such models are capable to predict the impact of air pollution on climate and air quality in future scenarios. In turn, the consistency allows to clearly attribute the observed concentration changes to the emission changes. This is particularly important since a central objective of the long-term regional monitoring programmes is to document changes in atmospheric composition and test the effectiveness of environmental policies. This work may demonstrate the usefulness of strengthening the international cooperation among regional measurement networks.

Results and Discussions

How have the changes in SO_2 emissions affected average regional sulfate concentrations?

The regional contributions to the global trends in sulfur emissions from 1990 to 2015 are illustrated with five year intervals in Fig. 1. The regional evolution of emissions are compared to annual average observed and modeled sulfate concentrations at the sites with measurements of sulfate in aerosols since 1990 (North America and Europe) or 2000 (East Asia). The model results are given as an ensemble mean from six global models. A complete statistical trend analysis of all the measured and modeled data of sulfate in aerosols, for several (sub-)periods is

Time period	Region	Nr. of stations	Average annual trend (STD) %/year		Absolute annual trend (STD) $\mu\text{gS}/\text{m}^3$ year	
			Obs	Ensemble	Obs	Ensemble
1980–1990	Europe	16	−2.56 (3.10)		−0.048 (0.094)	
1990–2000	Europe	41	−5.16 (2.11)	−5.23 (1.17)	−0.073 (0.052)	−0.070 (0.051)
1990–2000	North America	101	−2.08 (1.44)	−1.94 (0.43)	−0.024 (0.025)	−0.021 (0.014)
1990–2015	Europe	33	−2.93 (0.69)	−3.10 (0.48)	−0.031 (0.015)	−0.036 (0.023)
1990–2015	North America	124	−2.14 (0.67)	−2.19 (0.29)	−0.026 (0.024)	−0.024 (0.018)
2000–2010	East Asia	13	0.44 (4.25)	0.42 (1.15)	0.003 (0.034)	0.006 (0.013)
2000–2010	Europe	43	−2.86 (2.20)	−3.53 (1.06)	−0.029 (0.041)	−0.027 (0.017)
2000–2010	North America	227	−3.03 (1.72)	−3.22 (0.77)	−0.029 (0.029)	−0.027 (0.020)
2000–2015	East Asia	13	2.68 (9.41)	0.02 (0.91)	0.003 (0.037)	0.001 (0.009)
2000–2015	Europe	36	−2.67 (2.03)	−3.26 (0.85)	−0.025 (0.028)	−0.025 (0.015)
2000–2015	North America	218	−3.15 (1.30)	−3.18 (0.66)	−0.028 (0.029)	−0.024 (0.019)

Table 1. Average absolute and per cent trends in sulfate in aerosols. Data in bold indicate trends not consistent with the observations within the standard deviation (STD).

given in Table 1. The observations, emissions, and the model results show a consistent and substantial change in the regional sulfur budgets.

Globally the SO_2 emissions were reduced by 55 TgS (31%) from 1990 to 2015. Individual regions have had different contributions to the global emission budget throughout this period (see Fig. 1) as also documented in other studies^{1,14,21,25,37}. The largest decrease in global SO_2 emissions occurred in the first decade, from 1990–2000 and was mainly due to a large reductions in Europe (−42 TgS/−54%). There was a smaller decrease in North America (−7 TgS/−21%) during this time, and an increase in East Asia (+10 TgS/32%). In comparison, in the following period 2000–2015, emissions in Europe and the US decreased by a similar total amount (−14 and −13 TgS) or in relative terms, respectively by −40% and −50%. In Eastern Asia, there was an increase of the emissions up to 2005 by more than +20 TgS (70%), while in the last ten years from 2005 to 2015 there has been a reduction, we have used emission inventories with a decrease of −6 TgS (−13%). For the whole 25 year period from 1990 to 2015, India's emissions increased from 4.5 to 15 TgS, while in Africa only small changes occurred, +1 TgS (8%).

The emission inventories in China, which is the main contributor to the SO_2 emissions in East Asia, have been extensively studied the last years^{13,15–18,20,38}, and the most recent estimates indicate that the negative trends in the inventory used in our study is most likely underestimated. Zheng *et al.*²⁰ estimate SO_2 reduction in China of about 62% in the period 2010–2017, with the largest decrease after 2013 when the China's Clean Air Action was implemented. This rapid decline in the recent years appears to be confirmed with satellite observations^{20,23,39}. The main reason for these differences is that achieved effectiveness of policies implemented following China's Clean Air Action plans was not anticipated in earlier inventories. To illustrate the difference between the emissions used by the models in this study and the most recent estimates for the last ten year period in East Asia, the new inventories are included in Fig. 1, showing a decrease of −18 TgS (−34%) between 2005–2015^{18,20}, (shown as 'Alternative emissions').

The aerosol sulfate trends in observations and ensemble model results at the measurement sites with long term trends compare well with the trends of SO_2 emissions for all regions, especially North America and Europe (See Fig. 1). The ensemble model results and observations give comparable annual reductions of sulfate in aerosols by around 5.2%/y and 2.0%/y in Europe and North America, respectively, for the period 1990–2000 (Table 1). For the 2000–2015 period, the ensemble model and observations agree with 3.1%/y reduction in North America, while in Europe the ensemble model mean shows a higher relative reduction of 3.3%/y, compared to 2.7%/y in the observations, although the absolute changes are similar (−0.025 $\mu\text{gS}/\text{y}$, see Table 1), though the modelled and observed trends are comparable within the uncertainties for both relative and absolute changes per year.

The temporal development in East Asia was different with an increase in SO_2 emissions up to 2005, and a decline thereafter^{1,14,17,20,40}. The observations from this region do not capture the complete period, starting only in 2000, with relatively few sites. However they indicate the same tendency for an increase from 2000 to 2005 followed by a decline from 2005 to 2010. For the 2000–2010 period, both the ensemble model mean and the observations show a small average increase of 0.4%/y, although with quite high uncertainty, Table 1. There is an observed increase from 2010 to 2015, though it should be emphasized that the variability between the sites is high, and when considering that the emissions most probably have decreased more in the last five-year period, the increase in the observed sulfate concentrations seems to be non-representative. One should note that none of the sites with aerosols measurements used in this study are located in China. The large positive trend is mainly caused by two sites in Indonesia with 20–30% increases, which were not captured by the models. Whether this was due to local influence or long-range transport is difficult to say. It could be due to influences from volcanic activities in the region, but there does not seem to be an increase in eruptions the latter years⁴¹ nor do we see the same signal for the measured SO_2 .

Comparability between sulfur trends in gaseous phase, aerosols and wet deposition. The trends of SO_2 , sulfate in aerosols and sulfate in precipitation were compared using the EMEP MSC-W model result and the global observation set. It is important to note that the EMEP MSC-W model results are close to the ensemble mean for aerosol sulfate, as discussed in the next section. In addition to the measurement sites that provided long term observations of sulfate in aerosols (discussed above), observations of sulfate in precipitation

Time period	Region	Nr. of stations	Average annual trend (STD) %/year		Absolute annual trend (STD) kgS/ha year	
			Obs	EMEP MSC-W	Obs	EMEP MSC-W
1980–1990	Europe	23	−2.37 (2.33)		−0.30 (0.36)	
1980–1990	India	10	13.7 (25.6)		0.00 (0.18)	
1980–1990	North America	78	−1.80 (4.09)		−0.06 (0.18)	
1990–2000	East Asia (China)	3	−1.27 (2.67)	5.07 (0.36)	−0.16 (0.32)	0.68 (0.14)
1990–2000	Europe	60	−4.02 (4.44)	−6.41 (2.17)	−0.29 (0.29)	−0.91 (0.71)
1990–2000	India	10	22.6 (16.0)	4.31 (1.53)	0.42 (0.37)	0.18 (0.14)
1990–2000	North America	186	−1.84 (2.33)	−1.93 (0.48)	−0.10 (0.13)	−0.14 (0.11)
1990–2015	East Asia (China)	3	1.15 (0.74)	2.84 (0.23)	0.08 (0.05)	0.44 (0.11)
1990–2015	Europe	55	−3.03 (0.93)	−3.74 (0.49)	−0.16 (0.12)	−0.40 (0.26)
1990–2015	North America	189	−2.17 (0.65)	−2.41 (0.26)	−0.11 (0.10)	−0.19 (0.14)
2000–2010	Africa (Lamto)	1	4.15	2.69	0	0
2000–2010	East Asia	30	0.49 (4.14)	0.85 (2.01)	0.04 (0.37)	0.07 (0.28)
2000–2010	Europe	73	−3.85 (2.83)	−4.36 (1.22)	−0.16 (0.13)	−0.26 (0.19)
2000–2010	India	10	2.27 (8.48)	5.64 (2.21)	−0.07 (0.37)	0.29 (0.17)
2000–2010	North America	226	−2.30 (2.74)	−3.79 (0.68)	−0.12 (0.13)	−0.25 (0.19)
2000–2015	East Asia	30	−0.98 (2.48)	0.16 (1.33)	−0.12 (0.24)	0.05 (0.23)
2000–2015	Europe	67	−3.40 (1.37)	−3.94 (0.96)	−0.12 (0.10)	−0.23 (0.16)
2000–2015	North America	215	−2.78 (2.02)	−3.75 (0.65)	−0.13 (0.13)	−0.23 (0.18)

Table 2. Average absolute and per cent trends in wet deposition of sulfate. Data in bold indicate trends not consistent with the observations within the standard deviation (STD).

Time period	Region	Nr. of stations	Average annual trend (STD) %/year		Absolute annual trend (STD) $\mu\text{gS}/\text{m}^3$ year.	
			Obs	EMEP MSC-W	Obs	EMEP MSC-W
1980–1990	Europe	20	−5.03 (2.04)		−0.211 (0.168)	
1990–2000	Europe	43	−7.56 (1.81)	−8.54 (1.40)	−0.220 (0.275)	−0.318 (0.316)
1990–2000	North America	53	−3.27 (1.69)	−2.63 (0.30)	−0.125 (0.115)	−0.065 (0.037)
1990–2015	Europe	40	−4.43 (0.88)	−4.63 (0.43)	−0.084 (0.085)	−0.131 (0.132)
1990–2015	North America	71	−3.14 (0.75)	−2.83 (0.30)	−0.116 (0.109)	−0.066 (0.046)
2000–2010	Africa	8	17.6 (13.9)	1.86 (1.19)	0.144 (0.121)	0.012 (0.025)
2000–2010	East Asia	19	5.84 (9.40)	0.35 (2.22)	0.038 (0.119)	0.001 (0.025)
2000–2010	Europe	51	−4.23 (3.17)	−5.31 (1.61)	−0.046 (0.054)	−0.064 (0.055)
2000–2010	North America	78	−4.55 (1.68)	−4.44 (0.95)	−0.119 (0.113)	−0.080 (0.060)
2000–2015	Africa	8	4.97 (2.70)	1.11 (0.63)	0.062 (0.068)	0.008 (0.011)
2000–2015	East Asia	19	−0.14 (5.32)	−0.41 (0.92)	−0.055 (0.186)	−0.001 (0.031)
2000–2015	Europe	47	−3.89 (2.16)	−4.86 (1.31)	−0.036 (0.036)	−0.054 (0.046)
2000–2015	North America	77	−4.69 (1.35)	−4.40 (0.93)	−0.130 (0.123)	−0.069 (0.051)

Table 3. Average absolute and per cent trends in SO_2 . Data in bold indicate trends not consistent with the observations within the standard deviation (STD).

were available from sites in Africa, India, and additional Chinese sites (Table 2). For SO_2 , there was additional observational data from Africa (Table 3). Figure 2 shows the modeled global distribution of absolute and relative trends of concentrations and deposition. Comparing the maps with relative and absolute changes, the former visualize the trends better in areas where the concentrations or depositions are relatively low. This is especially visible in India where the relative changes are particularly large while the absolute changes are not, further note considerable positive trends from ship traffic, which has increased during the last decades^{1,14}.

Concentrations of the primary (directly) emitted compound, SO_2 , show greater decreases than the secondary (formed via atmospheric chemistry) sulfate in aerosols and in precipitation (Tables 1–3 and Figs S3–S5 in the SM). This non-linear relationship is seen in both model results and observations in North America and in Europe. This may partly be explained by the increasing oxidation capacity of the atmosphere during these twenty years^{7,42–44}. In the early 1990's, SO_2 emissions were still high, and the oxidation of SO_2 to sulfate was limited to some extent by the availability of the oxidants H_2O_2 , OH and O_3 . As the emissions decreased, more oxidants became available, and SO_2 was more efficiently oxidized to sulfate. Furthermore, a very important factor is that the decrease in SO_2 emissions (and only slightly decreasing ammonia emissions) has led to less acidic cloud droplets, which increased

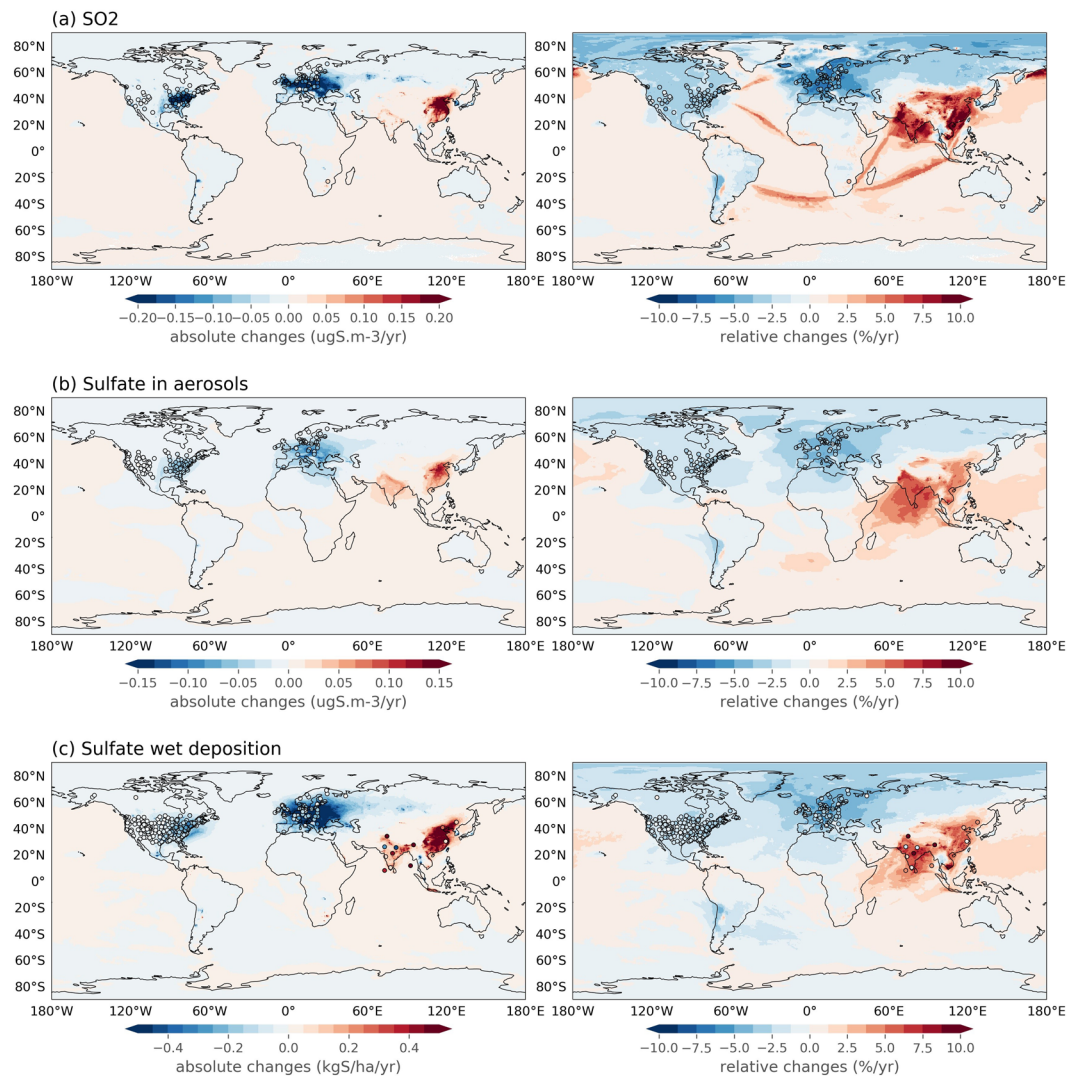


Figure 2. Absolute (left) and relative (right) trends of air concentrations and wet deposition calculated by the EMEP MSC-W model with observed trends superimposed (open circles), of SO_2 (a) and sulfate in aerosol (b) and wet deposition of sulfate (c) over the 1990–2015 period.

the oxidation rate of SO_2 to sulfate via the ozone pathway^{9,30,45}. In addition, less acidity in the environment probably leads to more efficient dry deposition of SO_2 ^{42,43,46}, which would also contribute to a larger reduction in SO_2 concentrations with respect to sulfate. The trends in wet deposition of sulfur are lesser than the trends in SO_2 , but larger than those of sulfate in aerosols, because both SO_2 and sulfate are efficiently scavenged by rain, and the wet deposition trend therefore represents a mix of SO_2 and sulfate in aerosols.

The somewhat puzzling increase in the observed sulfate concentration in aerosol seen in East Asia for 2010 to 2015 is not observed for SO_2 nor in sulfate in precipitation (Tables 1–3 and Figs S3–S5 in the SM). These show a steady decline from 2005–2015 and are more in line to the more recent inventories with a larger decrease in SO_2 emissions since 2010 period than the emissions used in the model calculations.

Comparability between the global models. The spatial variability in the aerosol sulfate trends calculated by the individual models for the whole period 1990–2015 is shown in Fig. 3, including also the ensemble model mean and the standard deviation between the models. The general pattern is quite well represented by all the models. Quantitatively, the models show very similar trends in North America and Europe, while in East Asia the spatial differences are larger. Notably some of the largest differences are found over the Himalayas, which is also the boundary between areas with upward and downward trends. Some of the differences between the models might be explained by how fast the models oxidize SO_2 and the lifetime of sulfate in aerosols⁴⁷.

When comparing the average relative trends of sulfate based on the observations and the models for different periods in Fig. 4 (the statistical information is found in Table S1 and S2 in the SM), the different models give similar trends as the observations, but there are systematic differences between them. NorESM gives the lowest relative reductions, while Sprintars and ECHAM6 generally give the highest reductions. The differences between the models are larger for Europe compared to North America, maybe due to fewer sites in Europe representing the region. For the modeled average relative trends for the regions defining the largest emission areas in North

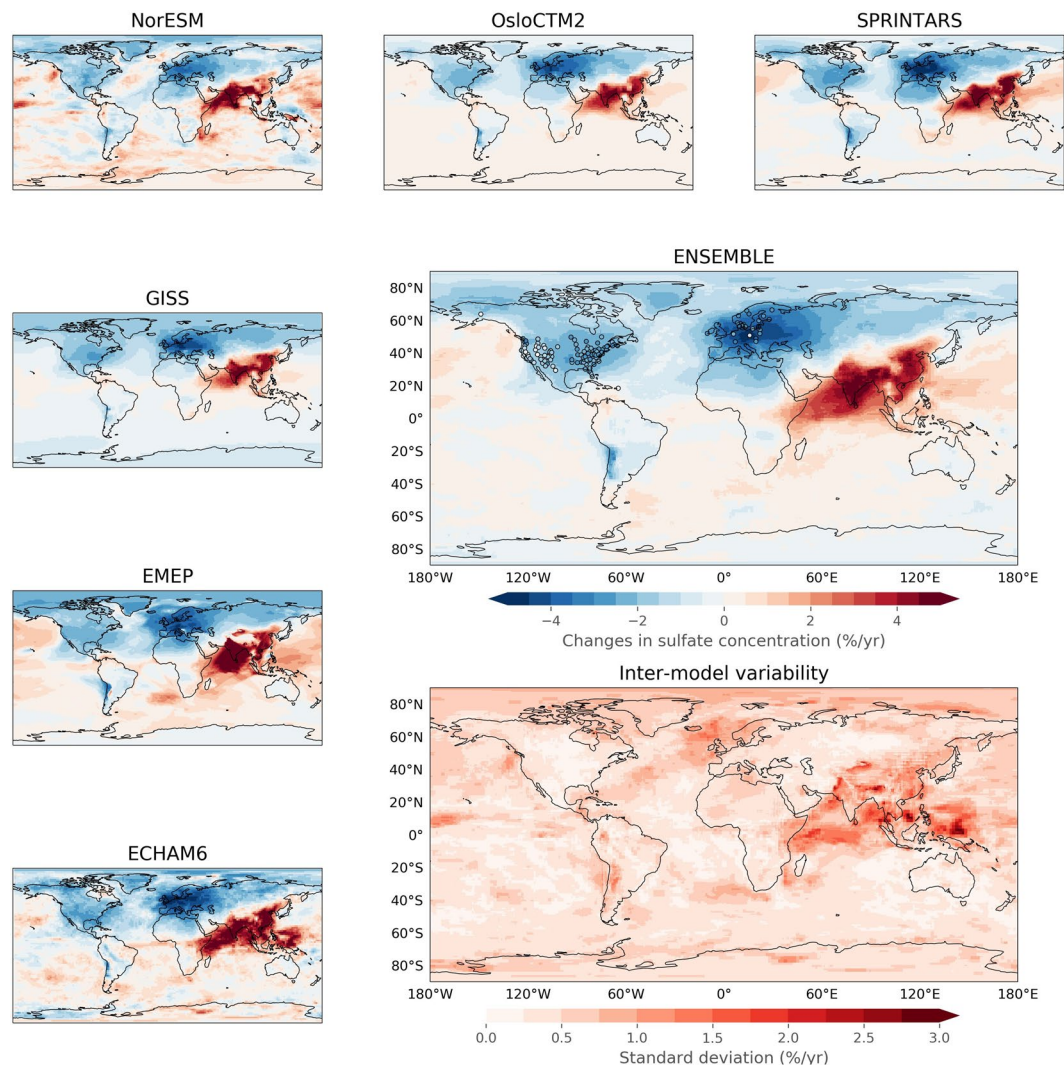


Figure 3. Relative trends in sulfate concentrations in aerosol for 1990–2015, calculated by the individual and ensemble models, with the observed trends superimposed (open circles). The differences between the models are shown in the inter-model variability map.

America and Europe, the systematic differences in the relative trends between the models are smaller (Fig. S6 in SM). When comparing the average concentrations for the regions, there is a large spread between the models, but the differences depend on how the regions are defined since the models show somewhat different spatial patterns.

Spatial representativeness of the regional trends. The number of sites needed to quantify and validate emission changes depends on both the spatial and temporal variability of the trends. This is true for both models and observations, but the variability in the measurements is higher (see box plot in Fig. S5 in SM), thus more difficult to detect significant trends. For example, in Europe, the models seem to simulate somewhat higher trend from 2000 onwards compared to the observations (see Fig. 4, Tables 1–3), although the differences are within the standard deviation. These variations can partly be explained by some sites with quite low concentration levels and high relative changes (though not necessarily significant trends), influencing the average relative trends. The models compare well with the trends at those sites with large significant reductions, which can be seen for the trends for the 25th percentile of the sites with the highest rate, with a change of $-4.1\%/y$ and $-3.8\%/y$ for the period from 2000 to 2015 for the ensemble model mean and observations for sulfate in aerosols, respectively.

In East Asia there are positive and negative trends depending on periods and components, while in India and Africa there are positive trends, but the variability in the observations are high and there are relatively few sites for all these three regions. The sites do not necessarily represent the whole regions. In Africa, SO_2 increases at a rate of $17 \pm 14\%/y$ from 2000 to 2010, but the increase occurred only in South Africa due to the influence of increased coal burning⁴⁸. At West- and Central African sites the concentrations are low and no significant trends are apparent, as reported earlier by Adon *et al.*⁴⁸. In China, there are three sites with precipitation measurements from 1990 on but, except for one site, these do not show the increase indicated by the models and by the emission trends for the 1990–2000 period. However, by extending the period to 2005, the sites indicate an increase, illustrating the sensitivity of the results to the choice of time period. In India the sites are quite well spread over

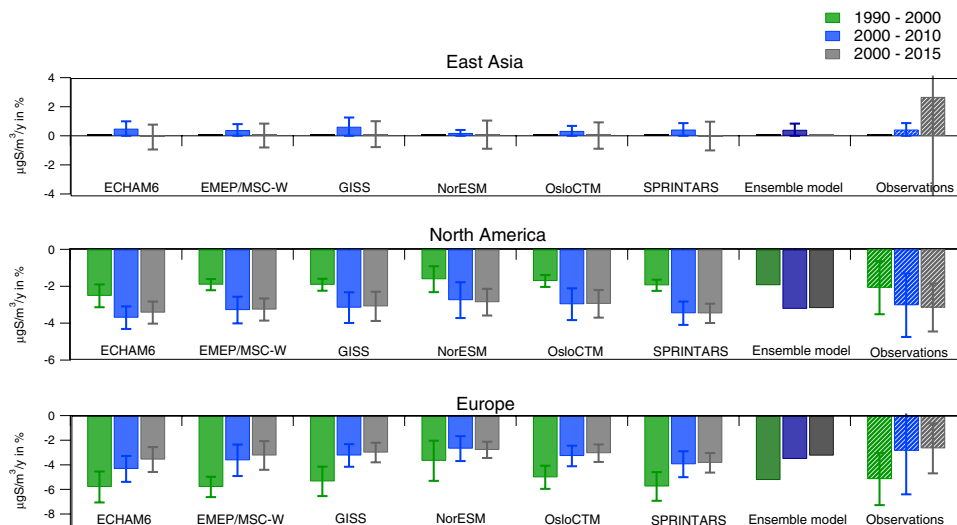


Figure 4. Comparison of the relative trends in sulfate concentrations in aerosol calculated by the different global models at sites with observed trends in the selected periods. The error bars indicate the standard deviation between the sites.

the country and there is a clear increase in the observed wet deposition in all the periods, which is also seen in the emissions and models. However, the magnitude of the trend is uncertain due to quite large variabilities and scattering in the time series.

A bootstrap approach has been used to assess how well the number of sites available represents each region. This is a possible method of assessing the representativeness of the trends, which, however, has its deficiencies. For example, changes in the absolute concentrations in North America, where most areas are remote, one is much more likely to pick a point in low rather than high concentration areas, while a large fraction of the observational sites are located closer to the higher emission and concentration regions. Thus the average observed concentrations are higher than in the bootstrap analysis results (Fig. S3 in SM). However, the standard deviation around the bootstrap mean is an indicator of the uncertainty caused by the geographical location of the given number of sites within each region. Figure 1 shows a high standard deviation of the sulfate concentrations in East Asia due to the relatively small number of sites and the inhomogeneous emission changes in this region.

For normalized trends (Fig. S4 in SM), the trends in the bootstrap averages are consistent with the modeled trends in North America for all the species, while in Europe the modeled trends at the sites are larger than the bootstrap average. This suggests that the site density in North America is representative for trend analysis for the whole region while in Europe the number of sites is apparently too low for a representative estimate. The normalized trends in emissions are most consistent with the trends in sulfate in aerosols, indicating that this is a relevant parameter for compliance monitoring. In East Asia, the normalized modeled trends from 1990–2005 show smaller increase than the bootstrap average, especially for SO_2 , which indicates that the sites are not located where the largest changes in the region have taken place, nevertheless the observations show larger changes for SO_2 and aerosol sulfate, though as discussed there are quite large variability between the sites in addition to the uncertainties in the emission inventory in this region.

Conclusions

The results give confidence in the global aerosol models' abilities to calculate historical sulfur trends and, thus, their scenario analyses of their future impact on climate and air quality. The fact that trends of emitted sulfur, sulfur in the aerosol phase after chemical transformation in the atmosphere, and sulfur in precipitation after wet removal agree between the observations and the model further implies that the relevant processes are realistically represented in the models.

However, one needs to be cautious when drawing conclusions from trends in regions with poor measurement site coverage, like India and China, and to some degree Africa, Australia and South America. There is a strong need for more sulfur observations in air, aerosols and precipitation to enable more homogeneous global coverage. Still, the work here reveals consistent trends on regional and global scales between the two independent methods. The good agreement also enhances confidence in the emission inventories in North America and in Europe and, in turn, confirms that the concentration changes are attributable to SO_2 emission changes. However, the bottom up emission inventory in East Asia used in this study has not captured the most likely large decrease in emissions in China after 2013. Further studies in this region require in depth comparison between updated emission inventories, atmospheric transport models, *in situ*- as well as satellite observations to better describe the significant changes in sulfur the last ten years for this region. The large ongoing increase in sulfur emissions in India also needs further investigations and should be more closely monitored.

This work has illustrated the strength of close co-operation between the regional networks to assemble a harmonized comparable global dataset. Future work on global trend analysis combining models and observations should include other species, in particular nitrogen compounds, organic and absorbing carbon are of high interest.

Acronym and references	Network	Region
CAPMoN ^{31,51}	Canadian Air and Precipitation Monitoring Network Including the New Brunswick Precipitation Network (NBPn), https://open.canada.ca/en/open-data	Canada
CASTNET ^{7,51}	Clean Air Status and Trends Network, https://www.epa.gov/castnet	US
EANET ^{31,51}	Acid Deposition Network in East Asia, http://www.eanet.asia/	East Asia
EMEP ^{10,11,31,51}	The European Monitoring and Evaluation Programme, http://ebas.nilu.no/	Europe
INDAAF ^{31,51}	International Network to study Deposition and Atmospheric chemistry in Africa, https://indaaf.obs-mip.fr/	Africa
IMPROVE ^{8,38}	Interagency Monitoring of Protected Visual Environments, http://vista.cira.colostate.edu/improve/	US
NADP ^{6,31}	National Atmospheric Deposition Program. Including data from MAP3S-AIRMoN (Atmospheric Integrated Research Monitoring Network), https://nadp.slh.wisc.edu	US
GAW - China	Global Atmosphere Watch, regional sites in China	China
GAW - India ^{26,31}	Global Atmosphere Watch, regional sites in India	India
WDCPC ³¹	WMO/GAW World Data Centre for Precipitation Chemistry, http://www.wdpc.org/	Global

Table 4. List of networks contributing with sites and data. The original data can be accessed from the given web pages.

Methods

Global dataset of sulfur observations. Measurement data were collected from different regional and global networks, in total 365 sites. A map showing the sites is found in Supplementary Fig. S1. More information on the networks, methods and access to original data can be found in the references and links given in Table 4.

Precipitation and wet deposition sulfate measurements are mainly from wet-only samplers or bulk samplers if proven comparable to wet-only and from similar sites as was described elsewhere³¹. The sulfate aerosol measurements are done using the aerosol filters, either PM₁₀ or no size cut off like the filterpack method, except for the IMPROVE network, which uses PM_{2.5} filters⁸. For SO₂, the filterpack method is commonly used in North America and Europe, while in Africa passive samplers dominate. In East Asia, both these methods in addition to continuous monitors are used. The sampling frequency is mostly daily and sometimes weekly, except for African data for which precipitation is sampled by event and SO₂ with monthly passive samplers. Wet deposition and volume-weighted precipitation data are based on the standard rain gauge depth if that is measured in parallel. At other sites without rain gauge, the sample precipitation amount is used. Monthly means are calculated for months with 70% or better data coverage. Urban sites are not included, and sites where the surroundings have changed considerably over the years have been excluded when known. The sites have been screened to be regionally representative with data of satisfactory quality.

Global modelling and emission estimates. The global models involved in the present study are described in Table 5. The model setup to simulate the sulfur changes varies between the models; from any fixed meteorology, to that of one particular meteorological year, to just fixed sea surface temperatures. All models simulated and diagnosed sulfate in aerosol, while only one model (EMEP/MSC-W) simulated SO₂ and wet deposition of sulfate for this study. In addition to sulfate, all the models simulated black carbon (BC) and primary organic aerosols (POA), and several also included secondary organic aerosols, nitrate, sea salt and dust. Details are found in Myhre *et al.*²⁵ and in the references in Table 5. All models use identical anthropogenic emission data from the EU project ECLIPSE for the 1990 to 2015 period; several updates and improvements compared to earlier emission data sets were included in this inventory^{21,49}. A direct link to the respective dataset is found here: <http://www.iiasa.ac.at/web/home/research/researchPrograms/air/ECLIPSEv5a.html>.

Natural emissions from i.e. volcanos are included but do vary somewhat between the models. See the references in Table 5 for details.

Statistical calculations. For each of the periods considered, the sites were selected based on the criteria that number of available years should be at least 75% of the total number of years in the period. The statistics are done from both yearly and seasonal averages, though only yearly are included. At least 10 measurements are required per season for being used in the statistics. The yearly averages are computed from the seasonally averages if the four seasonal averages are available (with more than 10 measurements) per year. Data from the same sites and periods have been extracted from the model output and trends have been calculated in similar way. Note that for most of the models (except NorESM and ECHAM6), there are only modelled data for each 5 year period. For the statistical analysis, the non-parametric Mann-Kendall test has been used on annual means for detecting and estimating trends; this is a common method when missing values occur and when data are not normally distributed^{10,11}. In parallel, the Theil-Sen's slope estimator has been used to quantify the magnitude of potential trends⁵⁰. A 90% confidence interval (p-value below 0.10) was chosen as the criterion for determining the significance of the trend. The Scientific Library for Python (scipy-0.14.0) has been used for calculating the trends. The average per cent changes are calculated for all the sites, not only for those with a significant trend. The robustness in the trends in modelled data for shorter periods (10–15 years) is hampered by having only few data point, i.e. 3 points for a ten year period. The Man Kendall test allows for calculation even down to 3 points, but with pval < 0.1 it is necessary with 4 points of more to estimate significance or not.

Models and references	Resolution	Fixed-met or fixed-SST
ECHAM6-HAM2 ^{52,53}	T63 1.8° × 1.8° L31	Climatological monthly varying fixed-SST and sea ice extent averaged for the period 1979 to 2008.
EMEP/MSC-W ⁵⁴	0.5° × 0.5° L20	2010 meteorology, 3 hourly ECMWF based
GISS ^{55,56}	2.0° × 2.5° L40	2000 climatological monthly varying fixed-SSTs and sea-ice
NorESM1 ^{57–59}	1.9° × 2.5° L26	Climatological monthly varying fixed SSTs and sea ice extent over the 1990–2013 period
OsloCTM2 ^{60,61}	T42 2.8° × 2.8° L60	2010 meteorology, 3 hourly ECMWF based
SPRINTARS ^{62,63}	1.125° × 1.125° L56	Climatological monthly varying fixed SSTs and sea ice extent over the 1988–1992 period

Table 5. Model descriptions.

To estimate how well the selected number of sites represents the trends in their region, a bootstrap approach was used. Using the same X number of observation sites, X arbitrary inland pixels were chosen and bootstrapped with 1000 iterations. The mean and standard deviation of these 1000 iterations were used to assess the representativeness of the monitoring networks.

Data Availability

The aggregated observational global data set with monthly mean concentrations and total wet deposition values, together with the model results at the same sites have, been associated with a specific DOI and can be downloaded from <https://doi.org/10.21336/gen.2>. The statistical results from all the individual time series are also available. A web tool, <http://aerocom.met.no/trends/S-trends/> maps the trends in SO₂ and sulfate in aerosol and wet deposition.

References

- Hoesly, R. M. *et al.* Historical (1750–2014) anthropogenic emissions of reactive gases and aerosols from the Community Emissions Data System (CEDS). *Geosci. Model Dev.* **11**, 369–408, <https://doi.org/10.5194/gmd-11-369-2018> (2018).
- Maas, R. & Grennfelt, P. E. (Eds.) *Towards Cleaner Air*. Scientific Assessment Report 2016, EMEP Steering Body and Working Group on Effects of the Convention on Long-Range Transboundary Air Pollution, https://www.unece.org/fileadmin/DAM/env/lrtap/ExecutiveBody/35th_session/CLRTAP_Scientific_Assessment_Report_-_Final_20-5-2016.pdf (Oslo, 2016).
- UNECE. *Towards Cleaner Air*. Scientific Assessment Report 2016: North America. https://www.unece.org/fileadmin/DAM/env/documents/2016/AIR/Publications/LRTAP_Assessment_Report_-_North_America.pdf (Geneva, 2016).
- Reis, S. *et al.* From Acid Rain to Climate Change. *Science* **338**, 1153–1154, <https://doi.org/10.1126/science.1226514> (2012).
- Vestreup, V., Myhre, G., Fagerli, H., Reis, S. & Tarrasón, L. Twenty-five years of continuous sulphur dioxide emission reduction in Europe. *Atmos. Chem. Phys.* **7**, 3663–3681, <https://doi.org/10.5194/acp-7-3663-2007> (2007).
- Lehmann, C. M. B., Bowersox, V. C., Larson, R. S. & Larson, S. M. Monitoring Long-term Trends in Sulfate and Ammonium in US Precipitation: Results from the National Atmospheric Deposition Program/National Trends Network. *Water, Air, & Soil Pollution: Focus* **7**, 59–66, <https://doi.org/10.1007/s11267-006-9100-z> (2007).
- Sickles, J. E. II & Shadwick, D. S. Air quality and atmospheric deposition in the eastern US: 20 years of change. *Atmos. Chem. Phys.* **15**, 173–197, <https://doi.org/10.5194/acp-15-173-2015> (2015).
- Hand, J. L., Schichtel, B. A., Malm, W. C. & Pitchford, M. L. Particulate sulfate ion concentration and SO₂ emission trends in the United States from the early 1990s through 2010. *Atmos. Chem. Phys.* **12**, 10353–10365, <https://doi.org/10.5194/acp-12-10353-2012> (2012).
- Banzhaf, S. *et al.* Dynamic model evaluation for secondary inorganic aerosol and its precursors over Europe between 1990 and 2009. *Geoscientific Model Development* **8**, 1047–1070, <https://doi.org/10.5194/gmd-8-1047-2015> (2015).
- Colette, A. *et al.* *Air pollution trends in the EMEP region between 1990 and 2012*, EMEP/CCC-Report 1/2016 <https://www.nilu.no/projects/ccc/reports/ccc1-2016.pdf> (Kjeller, 2016).
- Tørseth, K. *et al.* Introduction to the European Monitoring and Evaluation Programme (EMEP) and observed atmospheric composition change during 1972–2009. *Atmospheric Chemistry and Physics* **12**, 5447–5481, <https://doi.org/10.5194/acp-12-5447-2012> (2012).
- Crippa, M. *et al.* Forty years of improvements in European air quality: regional policy-industry interactions with global impacts. *Atmos. Chem. Phys.* **16**, 3825–3841, <https://doi.org/10.5194/acp-16-3825-2016> (2016).
- Saikawa, E. *et al.* Comparison of emissions inventories of anthropogenic air pollutants and greenhouse gases in China. *Atmos. Chem. Phys.* **17**, 6393–6421, <https://doi.org/10.5194/acp-17-6393-2017> (2017).
- Klimont, Z., Smith, S. J. & Cofala, J. The last decade of global anthropogenic sulfur dioxide: 2000–2011 emissions. *Environmental Research Letters* **8**, 014003 (2013).
- Zhang, Q., He, K. & Huo, H. Cleaning China's air. *Nature* **484**, 161 (2012).
- Li, M. *et al.* Anthropogenic emission inventories in China: a review. *National Science Review* **4**, 834–866 (2017).
- Li, M. *et al.* Comparison and evaluation of anthropogenic emissions of SO₂ and NO_x over China. *Atmos. Chem. Phys.* **18**, 3433–3456, <https://doi.org/10.5194/acp-18-3433-2018> (2018).
- Wang, J. *et al.* Particulate matter pollution over China and the effects of control policies. *Science of The Total Environment* **584–585**, 426–447, <https://doi.org/10.1016/j.scitotenv.2017.01.027> (2017).
- Xing, J. *et al.* Observations and modeling of air quality trends over 1990–2010 across the Northern Hemisphere: China, the United States and Europe. *Atmos. Chem. Phys.* **15**, 2723–2747, <https://doi.org/10.5194/acp-15-2723-2015> (2015).
- Zheng, B. *et al.* Trends in China's anthropogenic emissions since 2010 as the consequence of clean air actions. *Atmos. Chem. Phys.* **18**, 14095–14111, <https://doi.org/10.5194/acp-18-14095-2018> (2018).
- Klimont, Z. *et al.* Global anthropogenic emissions of particulate matter including black carbon. *Atmos. Chem. Phys.* **17**, 8681–8723, <https://doi.org/10.5194/acp-17-8681-2017> (2017).
- Saikawa, E. *et al.* Uncertainties in emissions estimates of greenhouse gases and air pollutants in India and their impacts on regional air quality. *Environmental Research Letters* **12**, 065002 (2017).
- Krotkov, N. A. *et al.* Aura OMI observations of regional SO₂ and NO₂ pollution changes from 2005 to 2015. *Atmos. Chem. Phys.* **16**, 4605–4629, <https://doi.org/10.5194/acp-16-4605-2016> (2016).
- Boucher, O. *et al.* *Clouds and Aerosols*. 571–657 (Cambridge, UK and New York, NY, USA 2013).
- Myhre, G. *et al.* Multi-model simulations of aerosol and ozone radiative forcing due to anthropogenic emission changes during the period 1990–2015. *Atmos. Chem. Phys.* **17**, 2709–2720, <https://doi.org/10.5194/acp-17-2709-2017> (2017).

26. Bhaskar, V. V. & Rao, P. S. P. Annual and decadal variation in chemical composition of rain water at all the ten GAW stations in India. *Journal of Atmospheric Chemistry* **74**, 23–53, <https://doi.org/10.1007/s10874-016-9339-3> (2017).
27. Itahashi, S. *et al.* A 15-year record (2001–2015) of the ratio of nitrate to non-sea-salt sulfate in precipitation over East Asia. *Atmos. Chem. Phys.* **18**, 2835–2852, <https://doi.org/10.5194/acp-18-2835-2018> (2018).
28. Berglen, T. F., Myhre, G., Isaksen, I. S. A., Vestreng, V. & Smith, S. J. Sulphate trends in Europe: are we able to model the recent observed decrease? *Tellus Series B-Chemical and Physical Meteorology* **59**, 773–786, <https://doi.org/10.1111/j.1600-0889.2007.00289.x> (2007).
29. Civerolo, K. *et al.* Evaluation of an 18-year CMAQ simulation: Seasonal variations and long-term temporal changes in sulfate and nitrate. *Atmospheric Environment* **44**, 3745–3752, <https://doi.org/10.1016/j.atmosenv.2010.06.056> (2010).
30. Paulot, F., Fan, S. & Horowitz, L. W. Contrasting seasonal responses of sulfate aerosols to declining SO₂ emissions in the Eastern U.S.: Implications for the efficacy of SO₂ emission controls. *Geophysical Research Letters* **44**, 455–464, <https://doi.org/10.1002/2016GL070695> (2016).
31. Vet, R. *et al.* A global assessment of precipitation chemistry and deposition of sulfur, nitrogen, sea salt, base cations, organic acids, acidity and pH, and phosphorus. *Atmospheric Environment* **93**, 3–100, <https://doi.org/10.1016/j.atmosenv.2013.10.060> (2014).
32. Rodhe, H., Dentener, F. & Schulz, M. The Global Distribution of Acidifying Wet Deposition. *Environmental Science & Technology* **36**, 4382–4388, <https://doi.org/10.1021/es020057g> (2002).
33. Bouwman, A. F., Van Vuuren, D. P., Derwent, R. G. & Posch, M. A Global Analysis of Acidification and Eutrophication of Terrestrial Ecosystems. *Water, Air, and Soil Pollution* **141**, 349–382, <https://doi.org/10.1023/A:1021398008726> (2002).
34. Dentener, F. *et al.* Nitrogen and sulfur deposition on regional and global scales: A multimodel evaluation. *Global Biogeochemical Cycles* **20**, n/a–n/a, <https://doi.org/10.1029/2005GB002672> (2006).
35. Tan, J. *et al.* Multi-model study of HTAP II on sulphur and nitrogen deposition. *Atmos. Chem. Phys. Discuss.* **2018**, 1–36, <https://doi.org/10.5194/acp-2017-1121> (2018).
36. Chin, M. *et al.* Multi-decadal aerosol variations from 1980 to 2009: a perspective from observations and a global model. *Atmos. Chem. Phys.* **14**, 3657–3690, <https://doi.org/10.5194/acp-14-3657-2014> (2014).
37. Smith, S. J. *et al.* Anthropogenic sulfur dioxide emissions: 1850–2005. *Atmos. Chem. Phys.* **11**, 1101–1116, <https://doi.org/10.5194/acp-11-1101-2011> (2011).
38. Wang, S. X. *et al.* Emission trends and mitigation options for air pollutants in East Asia. *Atmos. Chem. Phys.* **14**, 6571–6603, <https://doi.org/10.5194/acp-14-6571-2014> (2014).
39. Paulot, F., Paynter, D., Ginoux, P., Naik, V. & Horowitz, L. W. Changes in the aerosol direct radiative forcing from 2001 to 2015: observational constraints and regional mechanisms. *Atmos. Chem. Phys.* **18**, 13265–13281, <https://doi.org/10.5194/acp-18-13265-2018> (2018).
40. Kurokawa, J. *et al.* Emissions of air pollutants and greenhouse gases over Asian regions during 2000–2008: Regional Emission inventory in ASIA (REAS) version 2. *Atmos. Chem. Phys.* **13**, 11019–11058, <https://doi.org/10.5194/acp-13-11019-2013> (2013).
41. Carn, S. A., Fioletov, V. E., McLinden, C. A., Li, C. & Krotkov, N. A. A decade of global volcanic SO₂ emissions measured from space. *Scientific Reports* **7** <https://doi.org/10.1038/srep44095> (2017).
42. Fowler, D., Muller, J., Smith, R. I., Cape, J. N. & Erisman, J. W. Nonlinearities in source receptor relationships for sulfur and nitrogen compounds. *Ambio* **34**, 41–46, [https://doi.org/10.1639/0044-7447\(2005\)034\[0041:nisrrf\]2.0.co;2](https://doi.org/10.1639/0044-7447(2005)034[0041:nisrrf]2.0.co;2) (2005).
43. Monks, P. S. *et al.* Atmospheric composition change - global and regional air quality. *Atmospheric Environment* **43**, 5268–5350, <https://doi.org/10.1016/j.atmosenv.2009.08.021> (2009).
44. Dalsoren, S. B. *et al.* Atmospheric methane evolution the last 40 years. *Atmos. Chem. Phys.* **16**, 3099–3126, <https://doi.org/10.5194/acp-16-3099-2016> (2016).
45. Redington, A. L., Derwent, R. G., Witham, C. S. & Manning, A. J. Sensitivity of modelled sulphate and nitrate aerosol to cloud, pH and ammonia emissions. *Atmospheric Environment* **43**, 3227–3234, <https://doi.org/10.1016/j.atmosenv.2009.03.041> (2009).
46. Fowler, D. *et al.* Atmospheric composition change: Ecosystems-Atmosphere interactions. *Atmospheric Environment* **43**, 5193–5267, <https://doi.org/10.1016/j.atmosenv.2009.07.068> (2009).
47. Kristiansen, N. I. *et al.* Evaluation of observed and modelled aerosol lifetimes using radioactive tracers of opportunity and an ensemble of 19 global models. *Atmos. Chem. Phys.* **16**, 3525–3561, <https://doi.org/10.5194/acp-16-3525-2016> (2016).
48. Adon, M. *et al.* Long term measurements of sulfur dioxide, nitrogen dioxide, ammonia, nitric acid and ozone in Africa using passive samplers. *Atmos. Chem. Phys.* **10**, 7467–7487, <https://doi.org/10.5194/acp-10-7467-2010> (2010).
49. Stohl, A. *et al.* Evaluating the climate and air quality impacts of short-lived pollutants. *Atmos. Chem. Phys.* **15**, 10529–10566, <https://doi.org/10.5194/acp-15-10529-2015> (2015).
50. Gilbert, R. O. *Statistical methods for environmental pollution monitoring.* (Van Nostrand Reinhold, 1987).
51. Myhre, C. L. & Baltensberger, U. (Eds). *Recommendations for a Composite Surface-Based Aerosol Network.* GAW Report 207, <https://www.wmo-gaw-wcc-aerosol-physics.org/files/gaw-207.pdf> (Geneva, 2013).
52. Stevens, B. *et al.* Atmospheric component of the MPI-M Earth System Model: ECHAM6. *J. Adv. Model. Earth Sy.* **5**, 146–172, <https://doi.org/10.1002/jame.20015> (2013).
53. Zhang, K. *et al.* The global aerosol-climate model ECHAM-HAM, version 2: sensitivity to improvements in process representations. *Atmos. Chem. Phys.* **12**, 8911–8949, <https://doi.org/10.5194/acp-12-8911-2012> (2012).
54. Simpson, D. *et al.* The EMEP MSC-W chemical transport model - technical description. *Atmos. Chem. Phys.* **12**, 7825–7865, <https://doi.org/10.5194/acp-12-7825-2012> (2012).
55. Schmidt, G. A. *et al.* Configuration and assessment of the GISS ModelE2 contributions to the CMIP5 archive. *J. Adv. Model. Earth Sy.* **6**, 141–184, <https://doi.org/10.1002/2013ms000265> (2014).
56. Shindell, D. T. *et al.* Interactive ozone and methane chemistry in GISS-E2 historical and future climate simulations. *Atmos. Chem. Phys.* **13**, 2653–2689, <https://doi.org/10.5194/acp-13-2653-2013> (2013).
57. Bentsen, M. *et al.* The Norwegian Earth System Model, NorESM1-M - Part 1: Description and basic evaluation of the physical climate. *Geosci. Model Dev.* **6**, 687–720, <https://doi.org/10.5194/gmd-6-687-2013> (2013).
58. Iversen, T. *et al.* The Norwegian Earth System Model, NorESM1-M - Part 2: Climate response and scenario projections. *Geosci. Model Dev.* **6**, 389–415, <https://doi.org/10.5194/gmd-6-389-2013> (2013).
59. Kirkevåg, A. *et al.* Aerosol-climate interactions in the Norwegian Earth System Model-NorESM1-M. *Geosci. Model Dev.* **6**, 207–244, <https://doi.org/10.5194/gmd-6-207-2013> (2013).
60. Myhre, G. *et al.* Modelled radiative forcing of the direct aerosol effect with multi-observation evaluation. *Atmos. Chem. Phys.* **9**, 1365–1392 (2009).
61. Skeie, R. B. *et al.* Anthropogenic radiative forcing time series from pre-industrial times until 2010. *Atmos. Chem. Phys.* **11**, 11827–11857, <https://doi.org/10.5194/acp-11-11827-2011> (2011).
62. Takemura, T. *et al.* A simulation of the global distribution and radiative forcing of soil dust aerosols at the Last Glacial Maximum. *Atmos. Chem. Phys.* **9**, 3061–3073 (2009).
63. Takemura, T., Nozawa, T., Emori, S., Nakajima, T. Y. & Nakajima, T. Simulation of climate response to aerosol direct and indirect effects with aerosol transport-radiation model. *J. Geophys. Res.-Atmos.* **110**, D02202, <https://doi.org/10.1029/2004jd005029> (2005).

Acknowledgements

This study benefited from the Norwegian research council project #229796 (AeroCom-P3) and the European Union Seventh Framework Programme (FP7/2007–2013) project #282688 (ECLIPSE). Data providers from all the regional and global networks are greatly acknowledged for sharing and submitting their data to be used.

Author Contributions

W.A. has coordinated the study and prepared the observational data, while A.M. has been responsible for the statistical calculations, mapping and developing the web interface. G.M., S.T., H.F., M.S. and C.L.M. have been part of the core writing team. W.A., V.B., J.H., C.G.-L., P.S.P.R., A.S., R.V., C.M.N.L., K.S. and X.X. have provided data from the various networks, Z.K. has provided emission data and G.M., S.T., R.C., G.F., H.F., D.O., J.Q., D.S., R.B.S. and T.T. have provided model output.

Additional Information

Supplementary information accompanies this paper at <https://doi.org/10.1038/s41598-018-37304-0>.

Competing Interests: The authors declare no competing interests.

Publisher's note: Springer Nature remains neutral with regard to jurisdictional claims in published maps and institutional affiliations.



Open Access This article is licensed under a Creative Commons Attribution 4.0 International License, which permits use, sharing, adaptation, distribution and reproduction in any medium or format, as long as you give appropriate credit to the original author(s) and the source, provide a link to the Creative Commons license, and indicate if changes were made. The images or other third party material in this article are included in the article's Creative Commons license, unless indicated otherwise in a credit line to the material. If material is not included in the article's Creative Commons license and your intended use is not permitted by statutory regulation or exceeds the permitted use, you will need to obtain permission directly from the copyright holder. To view a copy of this license, visit <http://creativecommons.org/licenses/by/4.0/>.

© The Author(s) 2019